

# Scaphoid Fracture Patterns—Part One: Three-Dimensional Computed Tomography Analysis

Tessa Drijkoningen, MD<sup>1</sup> Amin Mohamadi, MD<sup>1</sup> Shai Luria, MD, PhD<sup>2</sup> Geert A. Buijze, MD, PhD<sup>3</sup>

<sup>1</sup> Hand and Upper Extremity Service, Massachusetts General Hospital, Harvard Medical School, Boston, Massachusetts

<sup>2</sup> Department of Orthopedic Surgery, Hadassah-Hebrew University Medical Center, Jerusalem, Israel

<sup>3</sup> Department of Orthopedic Surgery, Academic Medical Center, Amsterdam, The Netherlands

Address for correspondence Geert A. Buijze, MD, PhD, Hand and Upper Extremity Surgery Unit, Lapeyronie University Hospital, 371, avenue du Doyen Gaston Giraud 34295 Montpellier cedex 5, France (e-mail: g.a.buijze@amsterdamumc.nl).

J Wrist Surg 2019;8:441–445.

## Abstract

**Objective** Using three-dimensional (3D) computed tomography models of acute scaphoid fractures, we looked for differences between volumetric size of the fracture fragments, recognizable groups, or a shared common fracture area.

**Methods** We studied 51 patients with an adequate computed tomography scan of an acute scaphoid fracture using 3D modeling. Fracture surfaces were identified and fragment volumetric size of the fracture fragments was measured. A principal component analysis was used to find groups. Density mapping was used to image probable common fracture areas in the scaphoid.

**Results** Forty-nine of 51 fractures had a similar pattern. It was not possible to identify subgroups based on fracture pattern. The mean volumetric size of the fracture fragments of the proximal ( $1.45 \text{ cm}^3 \pm 0.49 \text{ cm}^3$  standard deviation [SD]) and distal fracture fragments ( $1.53 \text{ cm}^3 \pm 0.48 \text{ cm}^3$  SD) was similar. There was a single common fracture area in the middle third of the bone. In the distal third, there were no horizontal fractures through—but only directly proximal to—the tubercle suggesting that these would be best classified as distal waist fractures.

**Conclusion** Acute scaphoid fractures mainly occur in the middle third of the bone and tend to divide the scaphoid in half by volumetric size of the fracture fragments. There were two distinct grouping patterns: fractures through the proximal and middle third were horizontal oblique, whereas fractures of the distal third were vertical oblique. It seems that scaphoid fractures might be classified into proximal pole fractures, a range of waist fractures, and tubercle avulsion fractures.

**Level of evidence** This is a Level IV study.

## Keywords

- ▶ scaphoid fracture
- ▶ classification

If we can identify specific scaphoid fracture patterns, we might use different fixation strategies. For instance, a screw along the longitudinal axis of the scaphoid may be optimal if the fracture is 90 degrees to this axis, but fractures angled 50 to 55 degrees with respect to the longitudinal axis may be stabilized better by a slightly off axis screw.

To better understand scaphoid fracture appearance on radiographs, Compson evaluated 50 healthy scaphoid cadaver bones.<sup>1</sup> He then selected 10 bones that he felt represented important variations in pattern and anatomical features and made 10 clear methyl methacrylate models. Using radiographs of 91 scaphoid fractures, he then selected

received  
July 31, 2018  
accepted  
May 18, 2019  
published online  
July 8, 2019

Copyright © 2019 by Thieme Medical Publishers, Inc., 333 Seventh Avenue, New York, NY 10001, USA.  
Tel: +1(212) 584-4662.

DOI <https://doi.org/10.1055/s-0039-1693050>.  
ISSN 2163-3916.

a scaphoid model of appropriate pattern and size selected from the set of 10 models over radiographs and drew the fracture lines on the model. He found that 80 of the fractures could be captured in three different classes: the “surgical waist,” the dorsal sulcus, and the proximal pole. The dorsal sulcus fractures were described by Compson as fractures at 45° to the surgical waist and therefore to the long axis of the bone. The fractures did not follow the sulcus to the tip of the tuberosity, but crossed the palmar face to the scaphocapitate facet at the lateral apex of the dorsal ridge. He found three variations: the fracture line could pass proximally, distally, or on both sides of the apex.

Currently, we can create three-dimensional (3D) models of the scaphoid directly from computed tomography (CT) scans using a computer. Luria et al used 124 scaphoid models to study scaphoid fracture angle morphology using a precise computerized 3D technique. They classified 86 as waist fractures, 13 distal third, and 25 proximal third. Most fractures had a volar distal to dorsal proximal horizontal oblique inclination relative to the volar dorsal vector with a mean angle of 53 degrees for waist fractures.<sup>2</sup>

The purpose of this study was to distinguish the various groups of acute scaphoid fracture patterns using 3D models. The primary hypothesis was that the relative volumetric size of the fracture fragments would divide the scaphoid into two comparable fragments and that a shared common fracture area can be defined.

## Materials and Methods

### Selection of CT Scans

After our institutional review board approved the study, we performed a retrospective search of billing data to identify patients with a scaphoid fracture between January 2003 and December 2014 at 2 level I trauma centers. Using the International Classification of Diseases, Ninth Revision, Clinical Modification codes (814.01 for closed fracture and 814.11 for open fracture), we identified 1,064 patients with scaphoid fractures. Inclusion criteria were patients aged 18 years or older with a fracture of the scaphoid; a CT scan performed within 30 days of injury; CT scan available and slice thickness 1.25 mm or less and displaying the complete scaphoid bone.

A total of 51 patients (4 with proximal pole and 47 with scaphoid waist fractures) met the inclusion criteria. Our study sample consisted of 41 men and 10 women with a mean age of 33 years (standard deviation [SD] = 13). Twenty-five (51%) of the scaphoid fractures involved the right hand. Thirty-five of the fractures were nondisplaced, 16 were displaced. None of the fractures were comminuted. All displaced fractures were reduced to fit the template bone. The template bone was a 3D reconstructed, unfractured, healthy scaphoid. During our 3D modeling, all displaced fractures were reduced. Also 35 (69%) patients had an isolated scaphoid fracture; in 16 (31%) cases another bone in the wrist or hand was also fractured. Surgery was performed in 28 (55%) cases. Of all patients, two (4%) had a nonunion after conservative treatment.

### Modeling of Scaphoid Bone

We obtained the original Digital Imaging and Communications in Medicine (DICOM) files of selected CT scans through the Picture Archiving Communications System database of the 2 hospitals. The DICOM CT scans were loaded into 3D Slicer (Boston, MA), a software program used for analysis and visualization of medical images. CT scans are shown in the program in three different manners, namely transverse, sagittal, and oblique. The scaphoid was manually marked per CT slice on transverse, sagittal, and oblique CT slides to get closest to the true fracture. Paint effect was used to mark the scaphoid in two different colors and the threshold paint option was used to make sure only the scaphoid was marked. Voxels within the predefined threshold range (250–1760 Hounsfield units) were labeled and annotated as bone. After marking the two fracture fragments of the scaphoid on each CT cut, a 3D polygon mesh reconstructions of the two fracture parts was reconstructed.

### Fracture Surface

The 3D mesh reconstructions were imported into rhinoceros (McNeel, Seattle, WA) for further analyses. The volumetric size of the fracture fragments of scaphoid fracture fragments was measured using the standard volume command in rhinoceros. Subsequently, a template scaphoid bone was used to fit all 51 scaphoid fracture cases. The template bone was enclosed in a rectangular shaped box to standardize the position in space of every fracture. The articular surface area was marked with a polyline on the mesh reconstructions and measured using the area command after splitting the mesh surface with the applied polyline. After creating the fracture surfaces, the x, y, z coordinates were extracted per fracture plane and exported to excel. The mesh reconstructions in the scaphoid template were also visualized using density mapping. For the density mapping, all 3D reconstructed scaphoid bones were projected on each other (→ Fig. 1). The darker the color in the density map, the more fracture planes overlapped in that specific voxel. So, a lighter color means that less voxels of fracture planes overlapped in those voxels. Fractures location was defined geometrically according to the third of bone that involved the full or largest part of the fracture (e.g., if 70% of the fracture line involved the middle third and 30% the distal third, it would be classified as a middle third fracture).

### Statistical Analyses

Baseline characteristics of study patients were summarized with frequencies and percentages for categorical variables and with means and SDs for continuous variables. To calculate the proximity of the different fractures, we projected, for each subject, the fracture points onto the plane of the first two principal components, and also onto the vector orthogonal to this surface. The first projection provided an estimate of the fracture plane, and the second projection measured deviation from this plane. We centered the projected points for each subject and determined the smallest convex region containing these points (i.e., the convex hull), and also the boundary and area of this circumscribed region. We used the projection on the out-of-plane vector to check for nonplanar fractures, and a

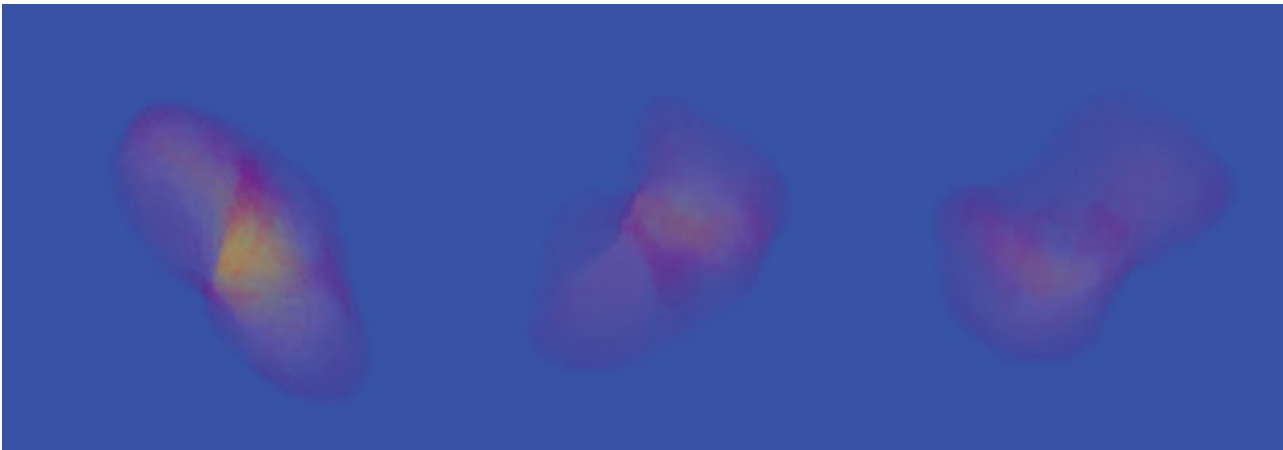


**Fig. 1** Density map of 51 scaphoid fractures.

plot of the superposition of the convex hull perimeters, centered at a common origin, to check for unusual fracture patterns. After removing outliers, we used hierarchical agglomerative clustering to attempt to cluster the fracture patterns.

## Results

Of the 51 fractures, 6 seemed to be proximal and 45 waist fractures. In our cohort, no distal fractures were found. Forty-nine of 51 fractures had a similar pattern (→ **Fig. 2**). It was not possible to identify subgroups based on fracture pattern. The mean volumetric size of the fracture fragments of the proximal fracture fragments was  $1.45 \text{ cm}^3$  ( $0.49 \text{ cm}^3$  SD) and the mean volumetric size of the fracture fragments of the distal fragments was  $1.53 \text{ cm}^3$  ( $0.48 \text{ cm}^3$  SD). Density maps also identified one similar horizontal oblique pattern of fractures, although we found an area in the middle of the scaphoid bone where most fractures were situated. We found six proximal pole fractures. Although several fractures were located directly proximal to distal tubercle, none of these fractures was (predominantly) located in the distal third of the scaphoid bone. Fractures were defined as distal if they were originated in the scapho-trapezio-trapezoid (STT) joint.

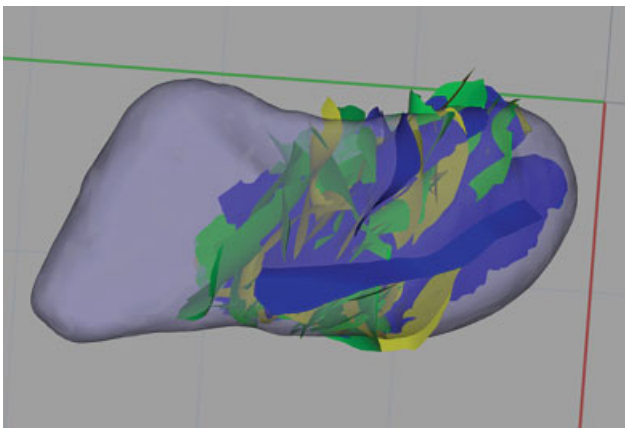


**Fig. 2** Fifty-one patients' fracture maps in rhinoceros.

## Discussion

This study showed that all scaphoid fractures in the proximal and middle third of the bone were similar horizontal oblique type fractures with a single common fracture area in the middle third of the bone. None of the most distal fractures went through—but only directly proximal to—the tubercle suggesting that these would be best classified as distal waist fractures. To investigate whether these notable findings were consistent with larger series, a secondary analysis of a similar previously published series of 124 scaphoid models was performed including 13 distal third fractures.<sup>2</sup> In this series of Luria et al comparable imaging techniques and definitions were used. In their series the distinct fracture patterns were identical—12 distal third fractures were oriented vertical oblique through the scaphoid tubercle, involving the STT joint (→ **Fig. 3**). This type of distal third fracture is more commonly referred to as a scaphoid tubercle fracture.<sup>3</sup>

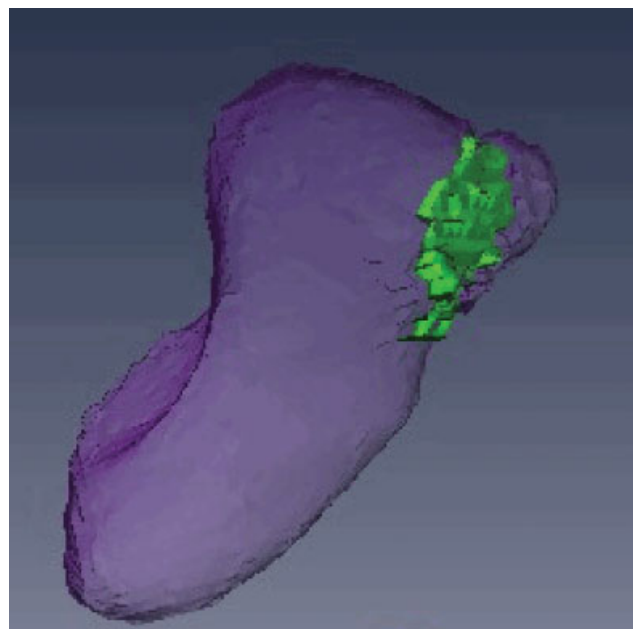


**Fig. 3** Scaphoid fracture map for tubercle fracture.

Scaphoid fractures are classified largely not only by location but also by displacement, fracture orientation, and healing stage.<sup>4</sup> It is not clear that there are distal third, nontubercle fractures that are distinct from waist fractures. Consistent with the series of Luria et al, we found that the vast majority of distal (pole) scaphoid fractures can be classified in two types according to whether or not they involve the tubercle: distal waist fractures (horizontal oblique directly proximal to the tubercle) and tubercle fractures (vertical avulsion type fractures through the tubercle). It is also difficult to draw a clear line between fracture of the proximal scaphoid and fractures of the scaphoid waist as there is no distinct pattern between these types of fractures. Using 3D-CT and fracture mapping, the vast majority of fractures were in the middle third of the bone and split the scaphoid in half by volumetric size of the fracture fragments.

Study limitations include the highly selective group of patients with a CT scan with a slice thickness 1.25 mm or smaller. This introduces sampling bias as the subset of patients may not be representative of the average patient with a scaphoid fracture. In particular, these fractures were likely either difficult to diagnose on radiographs or they were evaluated for the likelihood of displacement. Our impression is that these fractures are most representative of the subset of fractures that are more than a small distal tubercle fracture. The second limitation is that a healthy scaphoid was used as a template for mapping fractured scaphoids. There is significant variation in the size of the scaphoid, although this does not change the location of the fracture. This may have introduced a small amount of error and variation based on size of the scaphoid and alignment of the fracture, although scaphoid size should not necessarily affect the location of the fracture. For example, in our data, if the scaphoid was smaller, the fracture would still separate the bone in two comparable halves in volume of fracture fragments. In general, acute scaphoid fractures divide the scaphoid roughly in half by volumetric size of the fracture fragments. This is an interesting finding that to our knowledge has not been previously reported. It seems that there is less variation in fracture morphology and fracture size than previously imagined. As Compson noted, the variability on radiographs exaggerates the actual variability.<sup>1</sup> There seems to be a general mid-waist fracture area that divides the scaphoid roughly in half.

Although we did not find a statistically significant pattern, our density map shows the suggestion of a common fracture area in the middle third of the bone. This supports our thought that there is a continuous range of fractures in the middle third of the scaphoid bone rather than discrete categories (with exception of the tubercle fractures). Some of these might appear to involve the distal third depending on the position of the wrist and the projection of the radiographs. Patients with distal tubercle fractures uncommonly get CT scans, so none were included in this series. The current study shows that the vast majority of fractures can be classified on posteroanterior imaging of the scaphoid as (1) proximal pole fractures (proximal to the distal scapholunate (SL) interval), (2) a range of waist fractures (involving the scaphocapitate (SC)

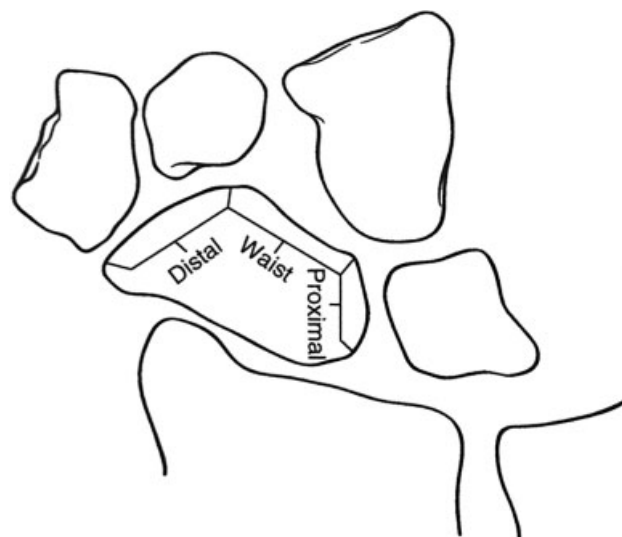


**Fig. 4** Simplified classification: distal, waist, and proximal pole fractures.

interval), and (3) distal tubercle fractures (involving the STT interval). Using this simplified anatomical classification system, the fracture is classified on posteroanterior radiographs based on the involvement of the adjacent joint interval as proximal (SL), waist (SC), or distal (STT) (► **Fig. 4**). Rarely, scaphoid fractures have been reported that do not fit this classification, such as coronal plane fractures and distal horizontal oblique fractures that seem to involve both the tubercle and the scaphocapitate interval.<sup>5,6</sup>

Many physicians have tried to classify and understand scaphoid fractures and their outcome using various techniques. Using fracture pattern, fracture fragment volumetric size of the fracture fragments, and density mapping in a 3D setting, we found a fracture area in the middle third of the bone but could not classify those fractures using the principal component analysis as all fractures through the proximal and middle third were horizontal oblique. There was only one distinct group of fractures of the distal third, which was vertical oblique described by Luria et al. It seems that scaphoid fractures might be classified into proximal pole fractures, a range of waist fractures, and tubercle avulsion fractures. A future study might compare plain film “assessment” of scaphoid fractures with CT scan volumetric fracture fragments as surgeons often judge scaphoid fracture patterns and fracture repair on radiographs alone.

#### Funding

None.

#### Conflict of interest

None declared.

#### Acknowledgments

The authors would like to thank Stein J Janssen and Mark Vanger for working on the statistics of this manuscript. They are grateful to David Ring for helping with the manuscript and Dirk ter Meulen for helping on the fracture mapping technique.

**References**

- 1 Compson JP. The anatomy of acute scaphoid fractures: a three-dimensional analysis of patterns. *J Bone Joint Surg Br* 1998;80(02):218–224
- 2 Luria S, Schwarcz Y, Wollstein R, Emelife P, Zinger G, Peleg E. 3-dimensional analysis of scaphoid fracture angle morphology. *J Hand Surg Am* 2015;40(03):508–514
- 3 Kraus R, Böhringer G, Meyer C, Stahl JP, Schnettler R. [Fractures of the scaphoid tubercle]. *Handchir Mikrochir Plast Chir* 2005;37(02):79–84 German.
- 4 Ten Berg PW, Drijkoningen T, Strackee SD, Buijze GA. Classifications of acute scaphoid fractures: a systematic literature review. *J Wrist Surg* 2016;5(02):152–159
- 5 Oron A, Gupta A, Thirkannad S. Nonunion of the scaphoid distal pole. *Hand Surg* 2013;18(01):35–39
- 6 Slutsky DJ, Herzberg G, Shin AY, et al. Coronal fractures of the scaphoid: a review. *J Wrist Surg* 2016;5(03):194–201